

Chronic Exposure to Environmental Concentrations of Tetrabromobisphenol A Disrupts Insulin and Lipid Homeostasis in Diet-Induced Obese Mice

Yi Ding, Tingfu Zhang, Hui-Bing Ma, Jian Han, Wenzhuo Zhu, Xiaolu Zhao, Xiao-Yi Lu, Bingsheng Zhou, and Xiong-Jie Shi*



Cite This: *Environ. Sci. Technol.* 2025, 59, 4330–4343



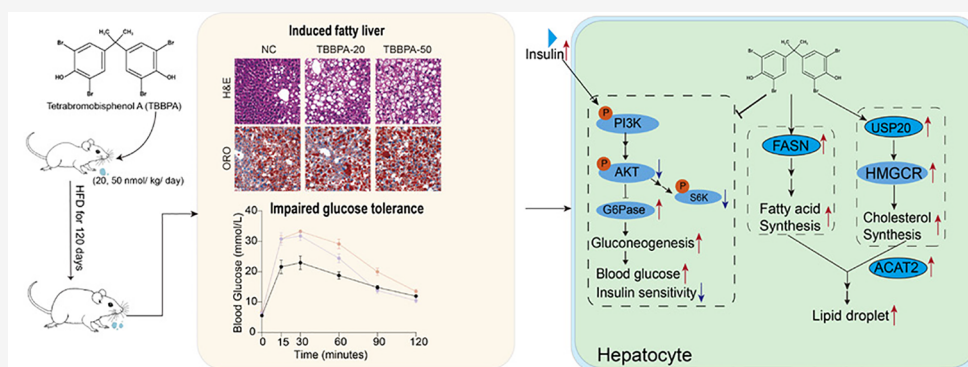
Read Online

ACCESS |

Metrics & More

Article Recommendations

Supporting Information



ABSTRACT: Tetrabromobisphenol A (TBBPA), a widely used brominated flame retardant in consumer products, has raised significant health concerns. However, the long-term metabolic effects of chronic exposure to environmentally relevant TBBPA concentrations, particularly in the context of modern high-calorie diets, remain poorly understood. Here, we show that C57BL/6J mice fed a high-fat diet and exposed to 20 or 50 nmol/kg/day TBBPA for 120 days exhibited increased body weight, aggravated fat accumulation, impaired glucose tolerance, insulin resistance, and dyslipidemia. Mechanistic investigations revealed that TBBPA exposure led to decreased norepinephrine levels, consequently reducing energy expenditure. It disrupts hepatic insulin signaling and upregulates G6Pase, thereby increasing the level of liver glucose production. Furthermore, TBBPA enhances hepatic cholesterol synthesis by elevating protein levels of HMGCR, which is the rate-limiting enzyme in cholesterol biosynthesis. This effect is mediated through increased expression of USP20, a specific deubiquitinating enzyme for HMGCR. Additionally, TBBPA modestly enhances fatty acid biosynthesis without significantly affecting lipolysis or fatty acid oxidation. Our research reveals novel molecular pathways through which environmental TBBPA exposure disrupts metabolic balance, potentially exacerbating obesity-related health issues. These findings highlight the synergistic effects between environmental pollutants and modern calorie-dense diets on metabolic health, emphasizing the importance of considering multiple factors in obesity-related disorders.

KEYWORDS: tetrabromobisphenol A, metabolic disruption, diet-induced obesity, insulin resistance, cholesterol biosynthesis

1. INTRODUCTION

Tetrabromobisphenol A (TBBPA), a brominated bisphenol A derivative, inhibits combustion through its bromine atoms, which scavenge reactive radicals at elevated temperatures, thereby disrupting flame propagation.¹ These properties have established TBBPA as the most extensively used brominated flame retardant, employed in over 70% of electrical and electronic products worldwide. The increasing consumer demand for printed circuit boards has significantly driven the demand for TBBPA.^{2–4}

The unbound TBBPA in products can readily leach into the environment due to its lack of chemical integration with the polymer matrix.⁴ TBBPA has been detected in various environmental matrices, including rivers, sediments, soil, and

urban outdoor air.^{3,5,6} As a lipophilic brominated flame retardant, TBBPA exhibits potential health and ecological risks due to its propensity for bioaccumulation, biomagnification, and environmental persistence.⁷ Recent studies indicate that TBBPA can enter the human body through multiple pathways, including dust ingestion, dermal contact, and dietary

Received: November 18, 2024

Revised: February 12, 2025

Accepted: February 19, 2025

Published: February 25, 2025



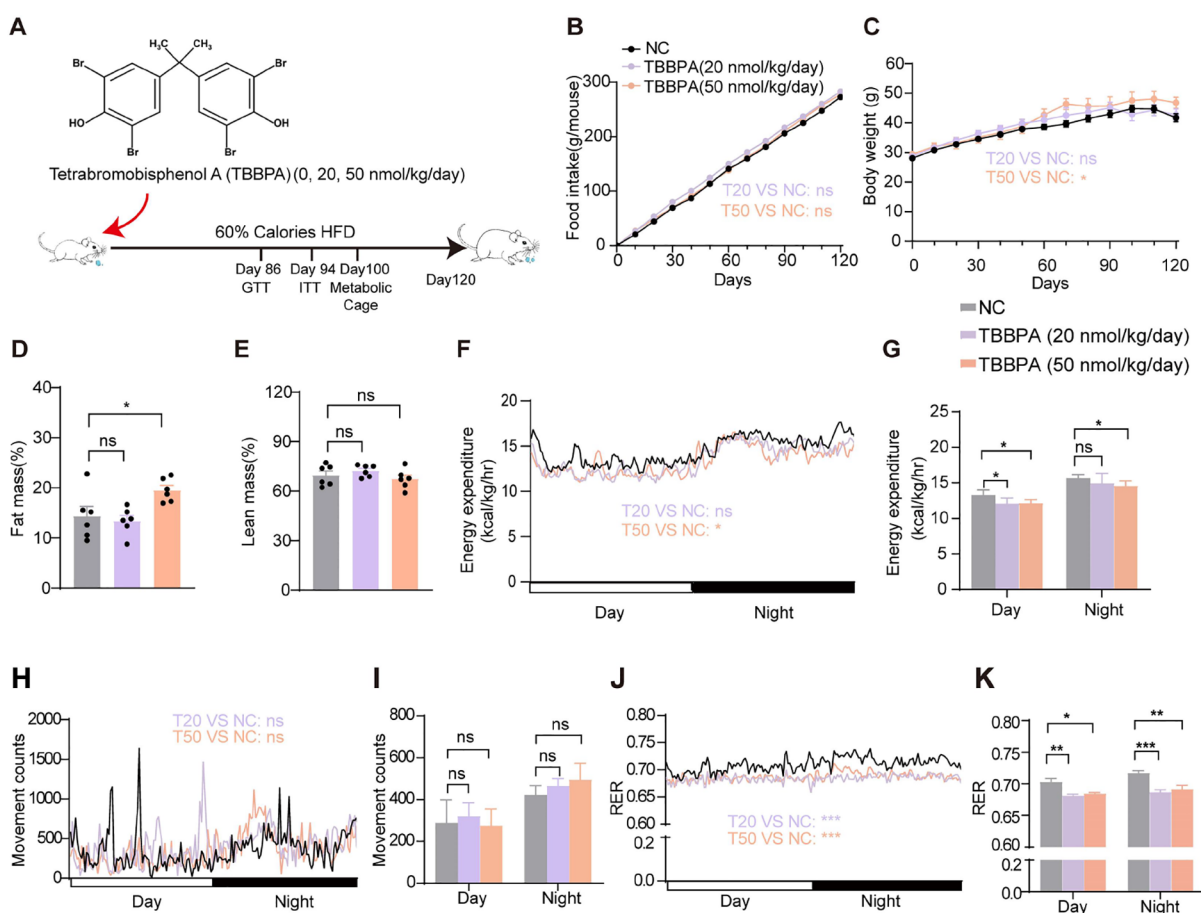


Figure 1. Effects of TBBPA exposure on metabolic parameters in mice fed a high-fat diet. (A) Schematic representation of the experimental design. Eight-week-old male CS7BL/6J mice were randomly assigned to treatment groups and fed a high-fat diet (60% calories from fat) containing various concentrations of TBBPA ($n = 6$). (B) Food intake throughout the experimental period. (C) Body weight over the course of the experiment. (D and E) Quantification of whole-body composition showing (D) fat mass and (E) lean mass. (F) Whole-body energy expenditure. (G) Average energy expenditure during day (07:00–19:00) and night (19:00–07:00). (H) Movement counts as determined by metabolic cages. (I) Average movement counts during day and night periods. (J) Respiratory exchange ratio (RER). (K) Average RER during day and night cycles. NC represents the negative control group. T20 and T50 represent the TBBPA exposure groups at 20 nmol/kg/day and 50 nmol/kg/day, respectively. Data are presented as mean values (B, F, H, J) or mean \pm SEM (C–E, G, I, K). Statistical analysis was performed using two-way ANOVA (B, C, F, H, J) or one-way ANOVA with Tukey's multiple comparison test (D, E, G, I, K). * $p < 0.05$, ** $p < 0.01$, *** $p < 0.001$ compared to the control group. ns: not significant.

intake.⁸ For instance, dust samples collected from residences in electronic waste recycling areas have revealed that the mean concentrations of TBBPA in indoor and outdoor dust are 3435 and 1998 ng/g-dw, respectively. Estimates of daily TBBPA exposure ranged from 0.04 to 7.50 ng/kg-bw in adults and 0.31 to 58.54 ng/kg-bw in children.⁹ TBBPA concentrations detected in breast milk samples have been reported to reach levels as high as 5124 pg/g lipid weight, with meat and meat products identified as the primary sources of TBBPA intake.¹⁰

While regulatory bodies continue to assess TBBPA's safety, several critical knowledge gaps and controversial points persist in understanding its health impacts. First, there is an ongoing debate about the significance of different exposure routes and their relative contributions to human health risks. Second, while acute toxicity studies have demonstrated clear endocrine-disrupting effects, the mechanisms underlying TBBPA's impact on metabolic homeostasis, especially under chronic exposure conditions, remain incompletely understood. The existing in vivo toxicological studies have demonstrated that TBBPA exerts endocrine-disrupting effects, capable of impacting thyroid hormonal, estrogen, insulin, and associated signaling

pathways.^{11–13} These hormones play crucial roles in modulating metabolic homeostasis through complex regulatory mechanisms. Consequently, alterations in the levels or activities of these hormones can lead to significant perturbations in lipid and glucose metabolism, potentially contributing to the development of metabolic disorders, such as obesity, diabetes, and dyslipidemia.¹⁴ Research has shown that even a single exposure to environmentally relevant levels of TBBPA is toxic to the liver, causing dysfunction and alterations in triacylglycerol and free fatty acid levels.¹⁵ Moreover, maternal exposure to TBBPA significantly alters the fecal microbiome and gut–liver axis in adult male offspring,¹⁶ highlighting the compound's far-reaching effects. In vitro experiments have also corroborated these findings, demonstrating that exposure to low concentrations of TBBPA can increase lipid and vitamin metabolic rates, leading to metabolic disorders in human hepatic cells.¹⁷

In the current era of industrialization and globalization, human dietary patterns have shifted toward more energy-dense, nutrient-poor foods.¹⁸ This dietary shift, coupled with an increasing imbalance of energy intake and expenditure, has

resulted in a rapid rise in the prevalence of overweight and obesity among adults and children worldwide.¹⁹ Overweight and obesity often impose additional metabolic stress, causing metabolic dysregulation and associated health issues, such as an increased risk of type 2 diabetes, nonalcoholic fatty liver disease, chronic kidney disease, and cardiovascular diseases.²⁰

While studies have explored the impact of TBBPA on glucose and lipid metabolism, the influence of chronic low-dose TBBPA exposure on these metabolic processes remains insufficiently characterized. To address this critical intersection of environmental exposure and metabolic health, our current study employed C57BL/6J mice as a model system. We aim to explore the metabolic effects of chronic exposure to environmentally relevant concentrations of TBBPA in the context of diet-induced obesity. Specifically, we investigate the impact of TBBPA on glucose and lipid metabolism under conditions of energy surplus pressure, seeking to elucidate the potential compounding effects of TBBPA on obesity-related metabolic dysregulation.

2. MATERIALS AND METHODS

2.1. Chemicals. TBBPA (catalog no. 330396; purity >97%) was obtained from Sigma (St. Louis, MO, USA). TBBPA was first dissolved in ethanol and subsequently mixed into a high-fat diet (HFD, 60% kcal/day from fat, Research Diets, D12492). The mixture was thoroughly homogenized, shaped into pellets, and finally dried overnight at 60 °C to remove ethanol. For the control group, an equal amount of ethanol was added to the food, followed by the same treatment. All other reagents used in this study were of analytical grade.

2.2. Mice Treatment. Male C57BL/6J mice were procured from the Center for Disease Control of Hubei, China. The mice were accommodated in colony cages within a pathogen-free environment, with the temperature maintained at 21–23 °C and relative humidity at 50–60%, while following a 12-h light/12-h dark cycle. Prior to the commencement of the study, all mice were provided ad libitum access to a standard chow diet (Research Diets, D10001). All experimental procedures involving animals were approved by the Institutional Animal Care and Use Committee (IACUC) of Wuhan University.

Eight-week-old male mice with comparable body weights were randomly divided into three experimental groups ($n = 6$ per group): a control group and two TBBPA treatment groups. At this time (week 8), all mice were switched from a standard chow diet to an HFD premixed with different concentrations of TBBPA. Mice were fed ad libitum; thus, TBBPA was administered orally through their diet. Based on the study by Yao et al., the environmentally relevant levels of TBBPA were calculated to be 57 nmol/kg body weight (bw).¹⁵ Additionally, environmental monitoring reveals TBBPA average concentrations of 672 $\mu\text{g/kg}$ in surface soils and up to 82.3 $\mu\text{g/kg}$ in sediments, while human exposure studies have documented levels of 37.34 $\mu\text{g/kg}$ lipid weight (lw) in maternal breast milk and 713 $\mu\text{g/kg}$ lw in infant serum.^{21–24} Taking these findings and the 120-day exposure duration into account, we established the dosing concentrations as 20 and 50 nmol/kg bw/day (≈ 68 and 170 $\mu\text{g/kg}$ TBBPA in diet). Body weight and food intake were recorded weekly after the experiment commenced. Glucose tolerance tests (GTTs) and insulin tolerance tests (ITTs) were conducted on days 86 and 94, respectively. Metabolic rates were assessed on day 100 using a

comprehensive laboratory animal monitoring system (CLAMS) developed by Columbus Instruments (Figure 1A). Measurements of VO_2 and VCO_2 were recorded over a 2-day period, with the initial 24 h serving as an acclimation period. The analyses were conducted under a 12-h light/12-h dark cycle at 23 °C. Body composition of mice was measured by time-domain nuclear magnetic resonance (TD-NMR) with a Bruker Minispec LF50 (Bruker Optics).

Upon completion of the 120-day exposure experiment, blood samples were obtained from the mice via retro-orbital collection after a 4 h fasting period to minimize the influence of food intake on metabolic parameters. Subsequently, the animals were euthanized by cervical dislocation. Immediately following euthanasia, organs were harvested, rapidly frozen in liquid nitrogen, and stored at -80 °C until analysis.

2.3. Immunoblotting. Mice tissues were homogenized in RIPA lysis buffer (50 mM Tris–HCl, pH 8.0, 150 mM NaCl, 2 mM MgCl_2 , 1.5% NP-40, 0.1% SDS, 0.5% sodium deoxycholate) supplemented with protease inhibitors (10 μM MG-132, 10 $\mu\text{g/mL}$ leupeptin, 5 $\mu\text{g/mL}$ pepstatin, 25 $\mu\text{g/mL}$ *N*-acetyl-leucinal-leucinal-norleucinal, and 1 mM dithiothreitol). Protein concentration was quantified using a BCA protein assay kit (Thermo Fisher Scientific). Equivalent amounts of proteins were separated by SDS-PAGE and transferred to polyvinylidene difluoride membranes. Membranes were blocked with 5% nonfat milk in Tris-buffered saline with Tween 20, followed by overnight incubation with primary antibodies at 4 °C. After washing, membranes were incubated with HRP-conjugated secondary antibodies at room temperature for 1 h. Immunoreactive bands were detected using a Pierce ECL Plus chemiluminescent substrate (Thermo Fisher Scientific). The antibodies used in this study are listed in Table S1. The specificity of all antibodies used has been validated either commercially or in our previous studies. Western blot band intensities were quantified using ImageJ software (version 1.53, National Institutes of Health, USA). All target protein bands were normalized to their corresponding loading control from the same blot to calculate the relative protein expression levels.

2.4. Glucose Tolerance and Insulin Tolerance Tests. Prior to the experiment, the mice were subjected to a fasting period of 16 h in preparation for the GTT or 4 h for the ITT. During the GTT, a dose of glucose corresponding to 2 g per kg of body weight was administered via intraperitoneal injection to the mice. For the ITT, an intraperitoneal injection of insulin at a dosage of 0.75 U per kg body weight was administered to the mice. The concentrations of glucose in tail blood were monitored at time points of 0, 15, 30, 60, 90, and 120 min postchallenge using a Onetouch Ultra glucose meter (Johnson & Johnson).

2.5. Blood and Liver Chemistry. Whole blood samples were allowed to clot at room temperature for 30 min, followed by serum separation via centrifugation at 1500g for 10 min. Hepatic tissues were homogenized in a methanol–chloroform mixture (2:1, v/v) and subsequently centrifuged to collect supernatants for lipid extraction. Total cholesterol and triglyceride concentrations were quantified using commercially available assay kits, following the manufacturer's prescribed protocols (Shanghai Kehua Bioengineering). Free fatty acid levels were enzymatically determined using the LabAssay NEFA kit (Wako, 294-63601). Glycerol levels were measured using an Amplex Red Glycerol Assay Kit (S0223S, Beyotime Biotechnology). Hepatic glycogen was visualized by periodic

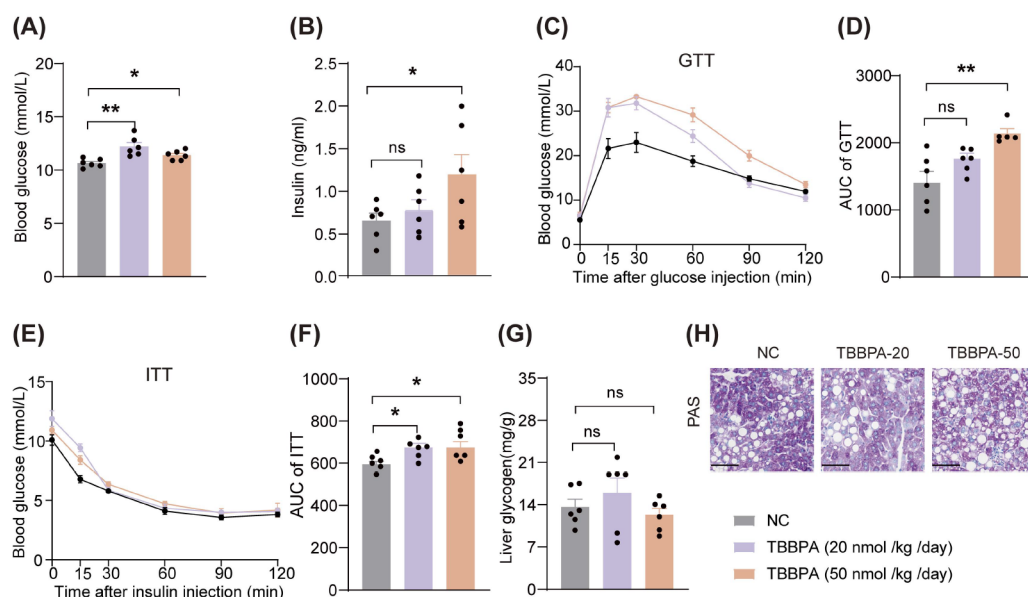


Figure 2. TBBPA enhances diet-induced glucose dysregulation. (A) Fasting blood glucose levels after 4 h of food deprivation. (B) Fasting serum insulin concentrations after 4 h of food deprivation. (C) Glucose tolerance test (GTT) performed on day 86 of high-fat diet feeding. (D) Area under the curve (AUC) analysis of GTT results shown in panel (C). (E) Insulin tolerance test (ITT) conducted on day 94 of HFD feeding. (F) AUC analysis of ITT results shown in panel (E). (G) Hepatic glycogen content measured after 120 days of HFD feeding. (H) Representative images of periodic acid-Schiff (PAS) staining of liver sections. Scale bars represent 100 μ m. NC represents the negative control group. TBBPA-20 and TBBPA-50 represent the TBBPA exposure groups at 20 and 50 nmol/kg/day, respectively. Data are presented as mean \pm SEM ($n = 6$). Statistical analysis was performed using one-way ANOVA with Tukey's multiple comparison test (B, C, D, F, G). * $p < 0.05$, ** $p < 0.01$ compared to the control group; ns: not significant.

acid-Schiff (PAS) staining (a kit from Pinuofei Biotechnology Co., following the manufacturer's protocol) and quantified using the Liver/Muscle Glycogen Assay Kit (A043-1-1, Nanjing Jiancheng Bioengineering Institute). Total bile acids were quantified using the TBA Kit (Shanghai Kehua Bioengineering Co.) Serum insulin concentrations were assessed using a mouse-specific insulin immunoassay kit (EZassay, MS100). Serum aspartate aminotransferase (AST) and alanine aminotransferase (ALT) activities were measured in accordance with the manufacturer's instructions (NJJCBIO, C009-2-1 for ALT, C010-2-1 for AST). Quantification of serum thyroxine (T_4), adrenaline, and noradrenaline levels was performed using enzyme-linked immunosorbent assay (ELISA) kits (Cloud Clone; CEA452Ge for T_4 , CEA858Ge for adrenaline, CEA907Ge for noradrenaline).

2.6. Quantitative PCR. Total RNA extraction from homogenized hepatic tissue was performed using Trizol Reagent (Invitrogen, 15596026), adhering strictly to the manufacturer's prescribed protocols. To eliminate potential genomic DNA contamination, the extracted total RNA was subjected to digestion with RNase-free DNase I (Promega, M6101). Subsequently, cDNA synthesis was carried out using 2 μ g of total RNA from each sample, employing M-MLV Reverse Transcriptase (Promega, M1701) for the reverse transcription process. Quantitative PCR (qPCR) analyses were performed using Hieff qPCR SYBR Green Master Mix (Yeasen Biotech, 11203ES), and the amplification profiles were assessed using a Bio-Rad CFX96. RNA expression levels were calculated by using the $\Delta\Delta C_t$ method. Primer sequences are listed in Table S2.

2.7. Statistical Analysis. Statistical analyses were carried out using GraphPad Prism 8 (GraphPad Software, Inc.). Data were first tested for normality using the Shapiro–Wilk test and homogeneity of variance using Levene's test. Data failing either

test underwent logarithmic transformation, followed by reassessment of both normality and variance homogeneity. Once these assumptions were confirmed, differences were analyzed using one-way or two-way ANOVA, as specified in the figure legends. A P value less than 0.05 was deemed to indicate statistical significance.

3. RESULTS AND DISCUSSION

3.1. TBBPA Exposure Alters Body Weight Gain and Energy Metabolism in Mice. Variations in body weight are widely recognized as a critical indicator for evaluating energy balance status.²⁵ Among groups with comparable food consumption levels, an upward trend increase in body weight was observed in the 20 nmol/kg/day treatment group, while a statistically significant increase was noted in the 50 nmol/kg/day treatment group compared to the control (Figure 1B,C). This observation suggests that TBBPA acts as an “obesogen”.²⁶ Specifically, mice exposed to 50 nmol/kg/day TBBPA exhibited an approximately 12.1% increase in body weight relative to the control group (Figure 1C). Multiple studies have established that a mere 5% gain in body mass significantly elevates various metabolic and cardiovascular risks.^{27,28} To further characterize these changes, we conducted detailed body composition analyses. The results revealed that mice in the 50 nmol/kg/day TBBPA group exhibited a significant increase in fat mass compared with the control group, while lean mass remained comparable among all groups with no statistically significant differences (Figure 1D,E). These findings suggest that the observed increase in body weight was primarily attributed to the accumulation of fat mass rather than changes in lean mass. Our investigation reveals that long-term TBBPA exposure may have potentially severe health ramifications.

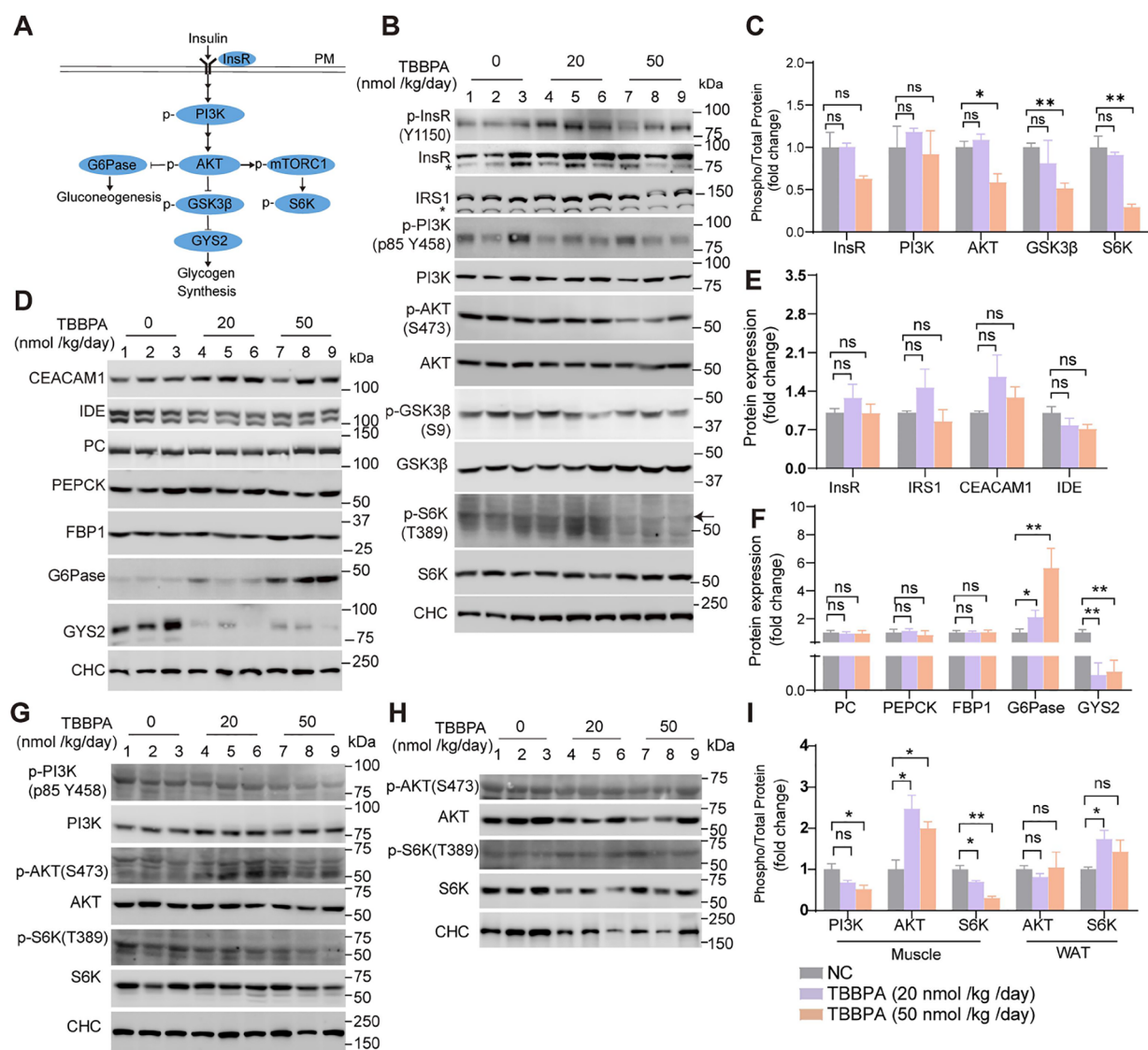


Figure 3. TBBPA exposure impairs hepatic insulin signaling and gluconeogenesis. (A) Schematic representation of insulin signaling pathway in the liver. PM represents the plasma membrane. Arrows indicate activation and perpendicular lines indicate suppression. (B) Representative immunoblots showing insulin signaling pathway proteins in tissue lysates from liver. Arrows indicate the bands corresponding to p-S6K. (C) Quantification of proteins related to insulin signaling pathway. (D) Immunoblots of proteins related to insulin degradation and glucose metabolism. (E, F) Quantification of immunoblots shown in panel (D). (G) Representative immunoblots showing insulin signaling pathway proteins in tissue lysates from skeletal muscle, and (H) white adipose tissue (WAT). (I) Quantification of immunoblots shown in panel (G, H). NC represents the negative control group. Data are presented as mean \pm SEM ($n = 6$). Statistical analysis was performed using one-way ANOVA with Tukey's multiple comparisons test (C, E, F, I). * $P < 0.05$, ** $P < 0.01$, ns: not significant.

To further investigate the metabolic implications of TBBPA exposure, we employed metabolic cages to evaluate alterations in energy expenditure (EE), locomotor activity, and respiratory exchange ratio (RER) in mice. Notably, our results demonstrated a significant decrease in EE among TBBPA-exposed mice across both diurnal and nocturnal periods (Figure 1F,G). Meanwhile, motion monitoring data indicated that TBBPA exposure did not significantly affect the mice's physical activity levels (Figure 1H,I). Energy expenditure encompasses four components: basal metabolic rate (BMR), the thermic effect of physical activity (TEPA), the thermic effect of food (TEF), and adaptive thermogenesis, with BMR being the most significant contributor, accounting for 60–75% of total energy expenditure.²⁹ Given the consistent housing conditions and physical activity levels maintained across all groups, it is reasonable to infer that TEPA, TEF, and adaptive

thermogenesis remained comparable between the control and exposed groups. Consequently, the reduced EE observed in TBBPA-exposed mice may be primarily attributed to alterations in the BMR.

Moreover, mice exposed to TBBPA exhibited significantly lower RER compared with the control group (Figure 1J,K). The control mice demonstrated an RER of 0.72, which is consistent with the high-fat diet they were fed. In contrast, both TBBPA-exposed groups showed RER values below 0.7. This observation suggests that the TBBPA-exposed mice may have experienced elevated levels of gluconeogenesis.³⁰ In summary, these findings indicate that TBBPA may act as a metabolic disruptor, potentially leading to changes in energy homeostasis and glucose metabolism.

3.2. TBBPA Exposure Impairs Glucose Homeostasis and Insulin Sensitivity. Following 120 days of TBBPA

exposure, mice in the treated groups exhibited elevated fasting blood glucose and insulin levels compared with the control group (Figure 2A,B). These findings collectively indicate that chronic exposure to TBBPA may induce a decrease in insulin sensitivity. To elucidate the impact of TBBPA exposure on glucose homeostasis, GTT and ITT were performed to evaluate glucose handling capacity and insulin sensitivity, respectively. GTT results revealed that mice exposed to TBBPA at doses of 20 and 50 nmol/kg/day exhibited a significantly more pronounced increase in blood glucose levels following intraperitoneal glucose administration (Figure 2C,D). Consistent with these findings, ITT results demonstrated that TBBPA exposure induced insulin resistance (Figure 2E,F). Our findings also align with previous studies that have linked exposure to bisphenols with insulin resistance and type 2 diabetes.³¹

In the liver, excess glucose is stored as glycogen, serving as a crucial energy reserve. To evaluate the impact of TBBPA exposure on hepatic glycogen content, we employed periodic acid-Schiff (PAS) staining along with biochemical analysis. Our findings revealed that exposure to TBBPA did not result in any significant alterations in the glycogen levels within the liver tissue of the mice (Figure 2G,H).

3.3. TBBPA Exposure Impairs Insulin Signaling and Induces Hepatic Gluconeogenesis. To delineate the underlying molecular mechanisms of glucose metabolic perturbations, we conducted an in-depth examination of the insulin signaling cascade. Insulin initiates its physiological effects by binding to the insulin receptor (InsR), which triggers a series of phosphorylation events, including the autophosphorylation of InsR and the subsequent activation of a complex network of downstream signaling proteins (Figure 3A). We assessed the phosphorylation status of key proteins in the hepatic insulin signaling pathway. TBBPA exposure did not alter the phosphorylation of InsR or phosphoinositide 3-kinase (PI3K); however, it resulted in a significant reduction in the phosphorylation levels of protein kinase B (AKT) and ribosomal protein S6 kinase (S6K) (Figure 3B,C). This suggests a substantial impairment of insulin signal transduction. Moreover, our findings revealed that TBBPA exposure did not modulate the protein expression of InsR, Insulin Receptor Substrate (IRS), and hepatic insulin clearance-associated proteins, such as carcinoembryonic antigen-related cell adhesion molecule 1 (CEACAM1) and insulin-degrading enzyme (IDE) (Figure 3D,E). This selective modulation implies a potential mechanism by which TBBPA attenuates hepatic insulin sensitivity without altering the insulin clearance kinetics. It is known that insulin signaling and its regulation constitute a highly intricate and complex process, involving numerous interconnected molecular pathways and feedback mechanisms.³² Therefore, the precise molecular targets of TBBPA within this complex network remain to be fully elucidated. Future studies should employ advanced techniques, such as phosphoproteomics and interactomics, to comprehensively map the disruption points within the insulin signaling network caused by TBBPA exposure.

Given the crucial role of the insulin signaling pathway in suppressing hepatic gluconeogenesis, we further investigated the expression of key gluconeogenic enzymes. Quantitative analysis of pyruvate carboxylase (PC), phosphoenolpyruvate carboxykinase (PEPCK), fructose-1,6-bisphosphatase 1- (FBP1), and glucose-6-phosphatase (G6Pase) protein expression revealed a dose-dependent significant increase in

G6Pase levels, the rate-limiting enzyme in gluconeogenesis, in the livers of TBBPA-exposed mice (Figure 3D,F). The liver plays a central role in whole-body glucose homeostasis by maintaining a delicate balance between glucose production and storage in the form of glycogen. Approximately 90% of endogenous glucose production is attributed to hepatic glucose production. Enhanced hepatic glucose production is a hallmark of insulin resistance and type 2 diabetes.³³ This upregulation of G6Pase suggests a potential mechanism by which TBBPA exposure may contribute to hyperglycemia and insulin resistance.

The insulin signaling pathway also plays a role in regulating glycogen synthesis. Activated AKT phosphorylates glycogen synthase kinase-3 β (GSK3 β), thereby regulating glycogen synthesis. Glycogen synthase 2 (GYS2) is a liver-restricted rate-limiting enzyme in glycogen synthesis. Our results demonstrate that mice exposed to TBBPA exhibited a significant decrease in the phosphorylation levels of GSK3 β in the liver, accompanied by a marked reduction in GYS2 protein expression (Figure 3B,C,D,F). However, we did not detect any changes in hepatic glycogen levels in the TBBPA-exposed group (Figure 2G,H). It is crucial to recognize that glycogen metabolism is a highly complex process that is regulated by multiple factors. The synthesis and utilization of glycogen are influenced by a variety of regulatory mechanisms, particularly under high-fat diet conditions.³⁴ Further studies will be required to comprehensively understand the impact of TBBPA on this metabolic pathway and to clarify how these molecular changes might affect glycogen dynamics in the context of metabolic disruption.

To further investigate the tissue-specific effects of TBBPA on insulin signaling, we examined the phosphorylation status of key signaling proteins in skeletal muscle and white adipose tissue (WAT). Intriguingly, TBBPA exposure elicited distinct tissue-specific responses in the insulin signaling cascade. In skeletal muscle, we observed a significant reduction in PI3K phosphorylation, accompanied by a paradoxical increase in AKT phosphorylation at Ser473 and decreased S6K phosphorylation (Figure 3G). In contrast, WAT exhibited a different response pattern with unchanged AKT phosphorylation levels but significantly elevated S6K phosphorylation (Figure 3H,I).

These tissue-specific alterations in insulin signaling components reveal a complex and heterogeneous response to TBBPA exposure across metabolically active tissues. The opposing effects on AKT phosphorylation between the liver (decreased) and muscle (increased) highlight the tissue-specific nature of TBBPA's impact on insulin signal transduction. The enhanced AKT phosphorylation in muscle, despite reduced PI3K activation, suggests the involvement of alternative regulatory mechanisms or compensatory pathways. Meanwhile, the elevated level of S6K phosphorylation in WAT, coupled with unchanged AKT activation, indicates potential AKT-independent regulation of S6K in adipose tissue. In addition, Castro et al. have demonstrated TBBPA's ability to dysregulate multiple receptor tyrosine kinases (RTKs), including EGFR, FGFR, and IGF1R, along with their downstream MAPK signaling in reproductive tissues,¹³ our findings reveal that TBBPA's effects on RTK signaling networks extend to metabolic regulation with remarkable tissue specificity. These findings underscore the complexity of metabolic regulation and suggest that TBBPA's effects on glucose homeostasis likely result from

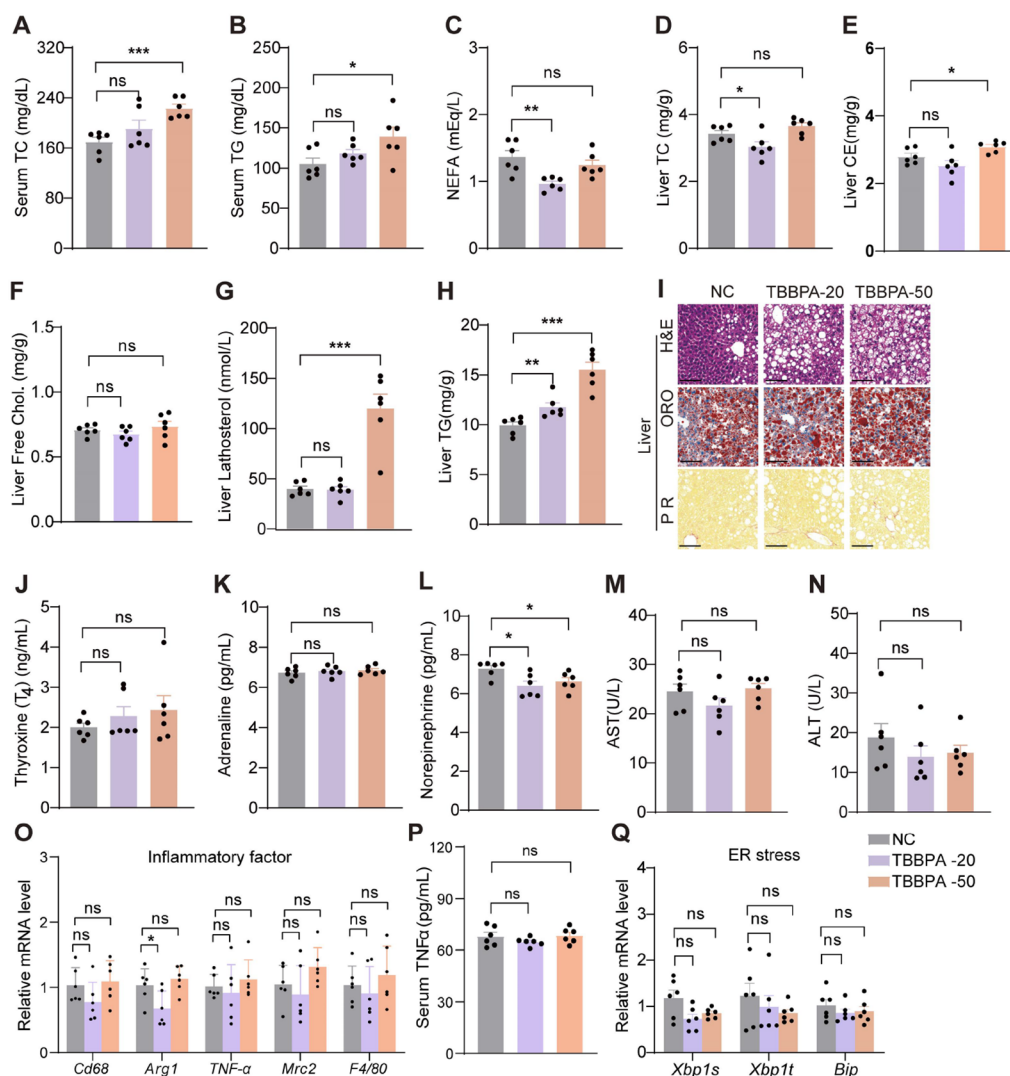


Figure 4. TBBPA treatment leads to disruptions in lipid homeostasis and endocrine function. (A) Serum total cholesterol. (B) Serum triglycerides. (C) Serum nonesterified fatty acids. (D) Hepatic levels of total cholesterol. (E) Hepatic levels of cholesteryl ester. (F) Hepatic levels of free cholesterol. (G) Hepatic levels of lathosterol. (H) Hepatic levels of triglycerides. (I) Representative images of liver sections stained with hematoxylin and eosin (H&E), Oil Red O, and Picrosirius Red (PR). Scale bars, 100 μ m. (J) Serum concentrations of thyroxine. (K) Serum concentrations of norepinephrine. (L) Serum concentrations of adrenaline. (M) Aspartate aminotransferase (AST) levels in serum. (N) Alanine aminotransferase (ALT) levels in serum. (O) Relative mRNA expression of inflammatory markers in liver tissue. (P) Serum concentrations of TNF α . (Q) Relative mRNA expression of ER stress markers in liver tissue. NC represents the negative control group. Data are presented as mean \pm SEM ($n = 6$). Statistical analysis was performed using one-way ANOVA with Tukey's multiple comparison test (A–H, J–Q). * $P < 0.05$, ** $P < 0.01$, *** $P < 0.001$. ns: not significant.

the integrated response of multiple tissues, each with distinct molecular alterations in the insulin signaling pathway.

Collectively, these findings provide evidence that TBBPA exposure disrupts glucose homeostasis through impairment of insulin signaling and dysregulation of hepatic glucose production.

3.4. TBBPA Exposure Induces Alterations in Lipid Metabolism and Hormonal Balance. To explore whether TBBPA exposure affects lipid metabolism, comprehensive biochemical analyses were conducted on serum and hepatic samples. Mice subjected to 50 nmol/kg/day TBBPA exhibited a marked elevation in serum total cholesterol (TC) and triglyceride (TG) concentrations (Figure 4A,B). Intriguingly, circulating nonesterified fatty acid (NEFA) levels displayed a declining trend, with a statistically significant reduction observed in the cohort exposed to 20 nmol/kg/day TBBPA

(Figure 4C). While hepatic TC and free cholesterol content remained unperturbed following TBBPA exposure, we observed significantly elevated levels of cholesteryl ester (CE) in mice exposed to 50 nmol/kg/day TBBPA. Additionally, a marked increase in hepatic lathosterol, a key intermediate metabolite in the cholesterol biosynthetic pathway, was detected in the same treatment group. The concurrent elevation of both lathosterol and CE levels provides compelling evidence of enhanced cholesterol biosynthesis and subsequent esterification in response to TBBPA exposure (Figure 4D–G). Notably, hepatic TG concentrations demonstrated a dose-dependent, significant increase (Figure 4H), suggesting TBBPA-induced perturbations in hepatic lipid metabolism. Hepatic histological analysis using hematoxylin and eosin (H&E) staining and Oil Red O (ORO) staining revealed increased lipid accumulation in the livers of mice

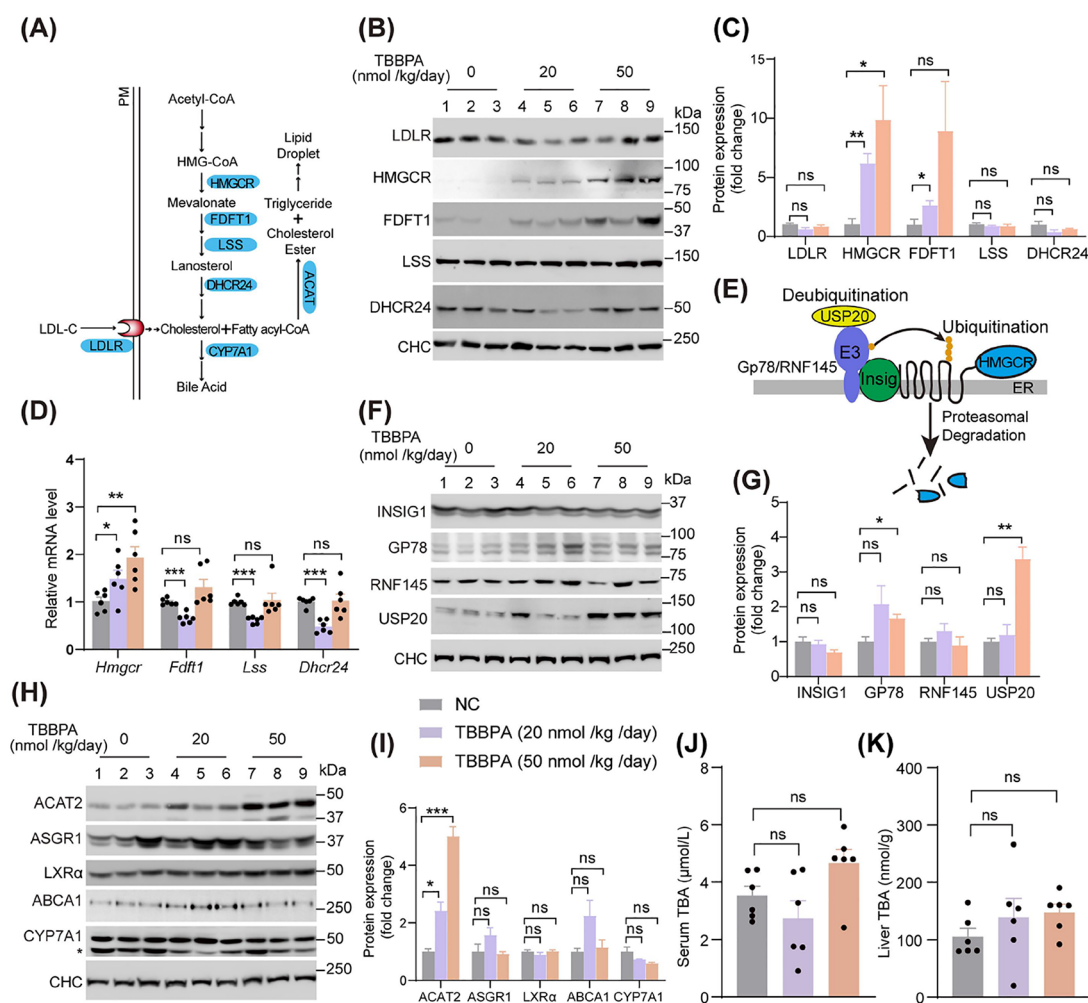


Figure 5. TBBPA promotes hepatic cholesterol synthesis via the USP20-HMGCR pathway. (A) Schematic representation of hepatic cholesterol metabolism pathways. PM represents the plasma membrane. (B) Immunoblots of proteins associated with cholesterol synthesis in liver lysates. (C) Quantification of immunoblots presented in panel (B). (D) Relative mRNA expression levels of genes involved in cholesterol biosynthesis in liver tissue. (E) Schematic representation of HMGCR protein stability regulation. HMGCR undergoes ubiquitination facilitated by the E3 ubiquitin ligases Gp78 or RNF145, in coordination with Insig, marking it for proteasomal degradation. USP20 acts as an HMGCR-specific deubiquitinating enzyme, stabilizing HMGCR by reversing its ubiquitination. (F) Immunoblots showing HMGCR ubiquitination- and deubiquitination-associated proteins in liver lysates. (G) Quantification of immunoblots presented in panel (F). (H) Immunoblots of cholesterol efflux-related proteins in liver lysates. (I) Quantification of immunoblots presented in panel (H). (J) Total bile acid concentrations in serum samples. (K) Total bile acid levels in liver tissue homogenates. NC represents the negative control group. Data are presented as mean \pm SEM ($n = 6$). Statistical analysis was performed using one-way ANOVA with Tukey's multiple comparison test (C, G, I–K). * $p < 0.05$, ** $p < 0.01$, *** $p < 0.001$. ns: not significant.

exposed to TBBPA (Figure 4I). Our assessment of hepatic fibrosis using Picrosirius Red staining, which specifically highlights collagen fibers, showed no significant increase in fibrosis levels in mouse liver following long-term TBBPA exposure (Figure 4I).

We further examined alterations in key hormones implicated in glucose and lipid homeostasis. Serum thyroid hormone (T_4) concentrations exhibited no statistically significant differences between the TBBPA-exposed and control cohorts (Figure 4J). While previous studies in aquatic models have demonstrated TBBPA's potential to disrupt thyroid hormone homeostasis, notably affecting T_3 and T_4 levels and their receptor expression patterns,^{11,12} our investigation revealed no significant alterations in serum T_4 levels following chronic TBBPA exposure in mice. This apparent discrepancy might reflect species-specific responses to TBBPA or differences in exposure conditions, suggesting that TBBPA's metabolic effects in mammals may

operate through mechanisms distinct from direct thyroid hormone disruption.

Interestingly, TBBPA exposure resulted in a significant reduction in circulating norepinephrine levels, while adrenaline concentrations remained unaffected (Figure 4K,L). Norepinephrine plays a pivotal role in modulating BMR, thereby enhancing oxygen consumption.³⁵ The observed decrease in norepinephrine levels could potentially lead to a reduced EE, a finding that aligns with our metabolic cage study observations (Figure 1F,G). In addition, norepinephrine is also a critical regulator of lipid metabolism, primarily acting through β -adrenergic receptors to stimulate lipolysis in the adipose tissue. In adipose tissue, this signaling cascade operates via cAMP-PKA activation, leading to the phosphorylation of hormone-sensitive lipase (HSL) and adipose triglyceride lipase (ATGL), which are essential enzymes for triglyceride breakdown.³⁶ The reduced norepinephrine levels observed in our study likely attenuate this lipolytic pathway, contributing to increased lipid

accumulation. Moreover, β -adrenergic signaling plays a crucial role in brown and beige adipose tissue activation and thermogenesis, processes intimately linked to lipid oxidation and energy expenditure.^{37,38} Consequently, the TBBPA-induced decrease in norepinephrine levels may impair BAT thermogenic capacity, further disrupting systemic lipid homeostasis. This is supported by our observations of increased body fat percentage, reduced energy expenditure, and increased hepatic lipid accumulation.

To evaluate potential TBBPA-induced hepatotoxicity, we measured serum activities of aspartate aminotransferase (AST) and alanine aminotransferase (ALT), which are established markers of liver injury. No elevation of AST or ALT levels was observed in TBBPA-exposed mice (Figure 4M,N). Additionally, the expression of inflammatory genes in the liver, including Cluster of Differentiation 68 (CD68), Arginase1 (*Arg1*), Tumor Necrosis Factor α (*TNF- α*), Mannose Receptor C-Type 2 (*Mrc2*), and Adhesion G Protein-Coupled Receptor E1 (*F4/80*), and serum *TNF- α* levels did not differ significantly between groups (Figure 4O,P). Given that endoplasmic reticulum (ER) stress can contribute to insulin resistance,³⁹ we examined the expression of canonical ER stress marker genes, including spliced X-box binding protein 1 (*Xbp1s*), total X-box binding protein 1 (*Xbp1t*), and binding immunoglobulin protein (*Bip*). Notably, these markers showed no significant alterations, indicating that TBBPA exposure did not induce ER stress (Figure 4Q). Collectively, these findings suggest that chronic exposure to environmentally relevant TBBPA levels does not precipitate overt hepatocellular damage or inflammatory responses.

3.5. TBBPA Exposure Enhances Hepatic Cholesterol Synthesis. To understand the mechanisms responsible for the observed elevation in serum TC following TBBPA exposure, we focused our investigation on the liver, the primary organ orchestrating cholesterol metabolism.⁴⁰ Hepatic cholesterol homeostasis is maintained through a delicate balance among cholesterol uptake, de novo cholesterol synthesis, and efflux pathways (Figure 5A). Initially, we assessed the expression of low-density lipoprotein receptor (LDLR) in the liver. LDLR is a major determinant of plasma cholesterol levels, mediating the uptake of LDL-cholesterol (LDL-C) from the circulation. Our results revealed no significant differences in hepatic LDLR protein levels between control and TBBPA-exposed groups, suggesting that variations in hepatic cholesterol uptake are unlikely to account for the observed differences in serum TC levels (Figure 5B,C). Subsequently, we conducted a comprehensive analysis of gene and protein expression profiles for key enzymes in the cholesterol biosynthesis pathway in murine hepatic tissue. Quantitative RT-PCR analysis revealed a significant 1.4-fold and 1.8-fold upregulation of 3-hydroxy-3-methylglutaryl-CoA reductase (*Hmgcr*) expression in the livers of mice exposed to 20 and 50 nmol/kg/day TBBPA (Figure 5D). Notably, Western blot analysis demonstrated an even more pronounced increase in HMGCR protein levels, with 6.2-fold and 9.8-fold elevations observed in the 20 and 50 nmol/kg/day TBBPA exposure groups, respectively (Figure 5B,C). The expression levels of farnesyl-diphosphate farnesyltransferase 1 (*Fdft1*), lanosterol synthase (*Lss*), and 24-dehydrocholesterol reductase (*Dhcr24*) exhibited a significant decrease of approximately 15–30% in the TBBPA-20 group, while remaining unaltered in the TBBPA-50 group (Figure 5D). However, the protein expression of DHCR24 and LSS showed no significant changes in either TBBPA-exposed mice group

(Figure 5B,C). The protein expression of FDFT1 showed a significant dose-dependent increase. These findings suggest that TBBPA may enhance hepatic cholesterol synthesis primarily by modulating the expression of HMGCR and FDFT1, with the regulatory effects predominantly occurring at the post-transcriptional level.

HMGCR is a rate-limiting enzyme in cholesterol biosynthesis. The regulation of HMGCR protein stability primarily involves ubiquitination and deubiquitination modifications (Figure 5E).⁴⁰ We examined the expression of proteins associated with HMGCR ubiquitination in the liver, including Glycoprotein 78 (Gp78), Ring Finger Protein 145 (RNF145), and Insulin-Induced Gene (Insig), as well as the deubiquitinating enzyme Ubiquitin Specific Peptidase 20 (USP20).⁴⁰ Intriguingly, only USP20 exhibited a significant increase in the level of protein expression (Figure 5F,G). USP20 is known to stabilize HMGCR through deubiquitination, preventing its proteasomal degradation. This mechanism may account for the observed increase in HMGCR protein expression in our study. Moreover, our observations revealed a notable increase in FDFT1 protein expression. Despite this finding, the current understanding of the regulatory mechanisms underlying FDFT1 protein expression remains limited. Future investigations are necessary to elucidate the precise pathways through which TBBPA influences the observed increase in FDFT1 protein levels. In sum, these findings suggest that TBBPA enhances cholesterol synthesis by increasing USP20 protein levels, which in turn stabilizes the HMGCR protein. Furthermore, our findings have significant therapeutic implications in the context of cardiovascular health. Given that cardiovascular disease remains the leading cause of mortality worldwide, and elevated cholesterol levels are a primary risk factor with a well-established causal relationship to cardiovascular events,⁴¹ the TBBPA-induced upregulation of cholesterol synthesis warrants particular attention. Clinical evidence has demonstrated that targeting cholesterol synthesis through HMGCR inhibition can reduce cardiovascular events by 22–24% for each millimole per liter reduction in LDL-C.⁴² Based on these established relationships, our findings suggest that inhibiting HMGCR enzyme activity via statins, or targeting USP20, either through the existing inhibitor GSK2643943A or siRNA-mediated knockdown, could potentially serve as a novel intervention strategy to mitigate TBBPA-induced cholesterol synthesis.⁴³

Acyl-CoA:cholesterol acyltransferase (ACAT) is a pivotal enzyme responsible for converting free cholesterol into CEs, which are subsequently stored in intracellular lipid droplets.⁴⁴ We observed a dose-dependent increase in hepatic ACAT (ACAT2) protein levels in mice exposed to TBBPA (Figure 5H,I). Previous studies have demonstrated that elevated cholesterol and fatty acid levels trigger cellular reactive oxygen species (ROS) production, leading to Cys277 oxidation and subsequent ACAT2 protein stabilization.⁴⁵ Moreover, increased ACAT2 expression has been shown to enhance CE secretion via apoB-containing lipoproteins.⁴⁶ Our findings reveal that TBBPA-exposed mice exhibited elevated hepatic TG, CE, and cholesterol synthesis, accompanied by increased serum TC and TG levels, while their hepatic TC and free cholesterol levels remained unchanged. Based on these observations, we propose a mechanistic model, wherein enhanced hepatic cholesterol synthesis promotes ACAT2 stabilization and potentially amplifies lipid accumulation (Figure 4I). Simultaneously, elevated ACAT2 levels facilitate

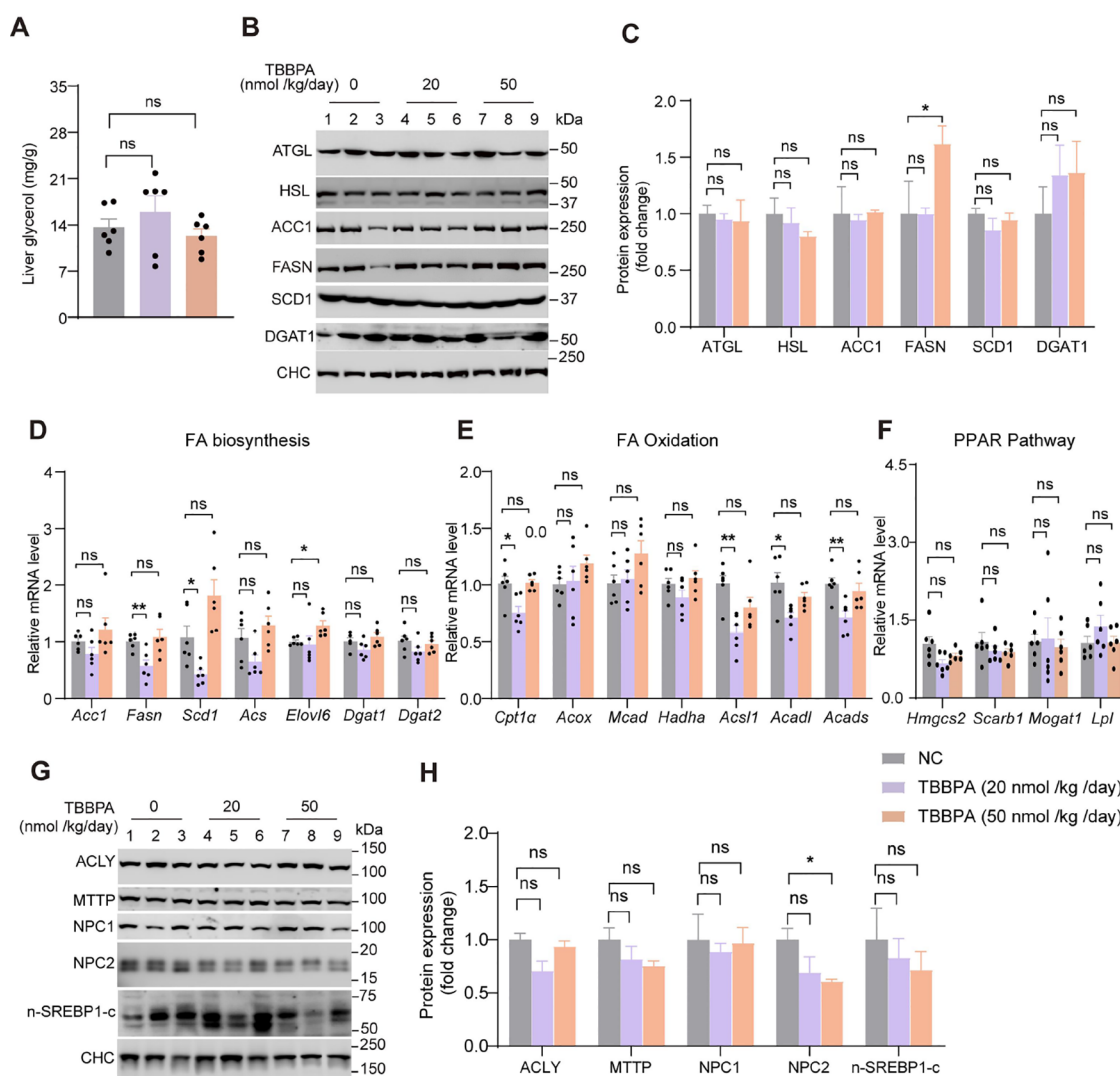


Figure 6. TBBPA exposure modulates hepatic lipid metabolism in mice liver. (A) Glycogen level in liver. (B) Immunoblots of proteins related to lipolysis and fatty acid synthesis in liver tissue. (C) Quantification of immunoblots presented in panel (B). (D) Relative mRNA expression levels of genes involved in hepatic fatty acid biosynthesis. (E) Relative mRNA expression levels of genes associated with hepatic fatty acid oxidation. (F) Relative mRNA levels of PPAR-regulated genes. (G) Representative immunoblots showing ACLY, MTTP, NPC1, NPC2, and nuclear SREBP-1C protein levels. (H) Quantification of immunoblots presented in panel (G). Data are presented as mean \pm SEM ($n = 6$). Statistical analysis was performed using one-way ANOVA with Tukey's multiple comparison test (C–F, H). * $p < 0.05$, ** $p < 0.01$. ns: not significant.

increased lipid secretion from the liver, resulting in elevated serum lipid levels without corresponding changes in hepatic free cholesterol content.

To exclude the possibility that TBBPA-induced hypercholesterolemia results from impaired cholesterol efflux, we examined the expression of Liver X Receptor (LXR) pathway genes and the expression of key proteins involved in cholesterol efflux, specifically Asialoglycoprotein Receptor 1 (ASGR1), LXR α , ATP-binding Cassette Transporter A1 (ABCA1), and Cholesterol 7 Alpha-Hydroxylase (CYP7A1). ASGR1 is known to regulate the stability of LXR α , which in turn enhances the expression of ABCA1 and ATP-binding Cassette Subfamily G Member 5/8 (ABCG5/G8). These transporters are critical for the transport of cholesterol to high-density lipoprotein and its excretion into bile.⁴⁷ CYP7A1 acts as the rate-limiting enzyme in the synthesis of bile acids, a major pathway for cholesterol elimination.⁴⁷ Our analysis revealed no significant differences in the hepatic expression of these proteins between control and TBBPA-exposed mice

(Figure 5H, part I). Consistent with these findings, serum total bile acid (TBA) and liver TBA levels remained unaltered following TBBPA exposure (Figure 5J,K). Thus, these findings suggest that TBBPA exposure does not impair hepatic cholesterol efflux or bile acid synthesis.

3.6. Impact of TBBPA on Hepatic Lipid Metabolic Processes. To delineate the mechanisms underlying TBBPA's effects on hepatic fatty acid metabolism, we investigated several core processes, such as lipolysis, triglyceride synthesis, fatty acid biosynthesis, and oxidation. No differences in hepatic glyceral levels (Figure 6A) or the expression of key lipolytic enzymes, hormone-sensitive lipase (HSL) and adipose triglyceride lipase (ATGL) (Figure 6B,C), were observed between the control and TBBPA-exposed groups, suggesting that TBBPA exposure does not interfere with lipolysis.

Subsequently, we examined the expression of genes and proteins associated with triglyceride synthesis and fatty acid biosynthesis in the livers of mice. Expressions of Acetyl-CoA Carboxylase 1 (*Acc1*), Fatty Acid Synthase (*Fasn*), Stearoyl-

CoA Desaturase (*Scd*), Acyl-CoA Synthetase (*Acs*), Diacylglycerol *O*-acyltransferase 1 (*Dgat1*), and *Dgat2* mRNA remained unchanged significantly (Figure 6D). However, the expression levels of Elongation of Very Long Chain Fatty Acid Protein 6 (*Elovl6*) mRNA were significantly increased in the group treated with 50 nmol/kg/day TBBPA (Figure 6D). Protein expression analysis revealed that only Fatty Acid Synthase (FASN) exhibited a slight increase, whereas ACC1, SCD, and DGAT1 showed no significant changes (Figure 6D,E). These findings suggest that TBBPA may modestly enhance lipid synthesis potentially through indirect regulatory mechanisms. Additionally, we examined the expression profiles of genes associated with fatty acid oxidation, including Carnitine palmitoyltransferase 1A (*Cpt1a*), Acyl-CoA oxidase (*Acox*), Medium-Chain acyl-CoA dehydrogenase (*Mcad*), Hydroxyacyl-CoA dehydrogenase trifunctional multienzyme complex subunit alpha (*Hadha*), Acyl-CoA synthetase long-chain family member 1 (*Acs1l*), Acyl-CoA dehydrogenase long chain (*Acadl*), and Acyl-CoA dehydrogenase short chain (*Acads*). While the mRNA expression levels of *Cpt1a*, *Acs1l*, *Acadl*, and *Acads* were downregulated significantly in the 20 nmol/kg/day TBBPA exposure group, the expression of all investigated genes remained unaltered significantly in response to 50 nmol/kg/day TBBPA exposure.

Given the pivotal role of the peroxisome proliferator-activated receptor (PPAR) signaling pathway in lipid metabolism regulation, and the possibility that TBBPA may act as a PPAR ligand,⁴⁸ we investigated whether PPARs serve as molecular targets of TBBPA. To this end, we examined the expression profiles of PPAR-regulated genes, including 3-Hydroxy-3-methylglutaryl-CoA synthase 2 (*Hmgcs2*), Scavenger receptor class B, member 1 (*Scarb1*), Monoacylglycerol *O*-acyltransferase 1 (*Mogat1*), and Lipoprotein lipase (*Lpl*). Analysis revealed no significant alterations in the expression levels of these target genes between the TBBPA-exposed and control groups (Figure 6F). These findings suggest that TBBPA-mediated perturbations in lipid metabolism likely occur through PPAR-independent mechanisms.

To gain deeper insights into the impact of TBBPA on hepatic lipid metabolic regulation, we examined the expression of key proteins involved in glucose-lipid metabolism and lipid transport. ATP citrate lyase (ACLY), a crucial metabolic hub enzyme that links glucose metabolism to lipid synthesis,⁴⁹ showed no significant changes in expression following TBBPA exposure. We further investigated the expression of proteins essential for lipid transport, including microsomal triglyceride transfer protein (MTTP), Niemann-Pick type C1 (NPC1), and Niemann-Pick type C2 (NPC2).⁵⁰ While MTTP and NPC1 expression remained unchanged, NPC2 expression was significantly decreased in the 50 nmol/kg/day TBBPA exposure group. Additionally, we assessed the nuclear form of SREBP-1C (n-SREBP-1C), a master regulator of lipogenic gene expression, and found no significant differences between the exposed and control groups (Figure 6G,H).

ACLY catalyzes the conversion of citrate to acetyl-CoA, providing essential substrates for de novo lipogenesis and cholesterol biosynthesis.⁴⁹ The unchanged expression of ACLY suggests that TBBPA's effects on metabolic homeostasis may not primarily operate through alterations in the citrate-dependent lipogenic pathway. Similarly, the maintained expression of n-SREBP-1C indicates that TBBPA exposure does not significantly alter the canonical lipogenic transcriptional program. However, the selective reduction in NPC2

expression, without concurrent changes in MTTP or NPC1, points to a specific vulnerability in the intracellular cholesterol trafficking pathways. NPC2 plays a crucial role in facilitating cholesterol transport from late endosomes/lysosomes to other cellular compartments, and its downregulation might contribute to altered cellular cholesterol distribution and subsequent metabolic dysfunction.⁵⁰ This selective effect on NPC2 suggests that TBBPA might primarily impact specific aspects of intracellular lipid trafficking rather than causing a broad disruption of lipid metabolic pathways.

Taken together, our data demonstrate that TBBPA exposure may selectively influence hepatic lipid metabolism by enhancing fatty acid biosynthesis without affecting lipolysis or fatty acid oxidation. This selective modulation of lipid metabolic pathways may contribute to the observed alterations in hepatic lipid profiles. It is important to note, however, that the regulatory effect of TBBPA on fatty acid biosynthesis appears to be relatively modest. This observation suggests that alternative regulatory mechanisms may be involved in mediating TBBPA's effects on hepatic lipid metabolism.

Our findings reveal a previously unrecognized mechanism underlying TBBPA-induced dyslipidemia, centered on post-transcriptional regulation of cholesterol synthesis through USP20-mediated HMGCR stabilization. While previous studies have demonstrated TBBPA's ability to disrupt hepatic lipid homeostasis through Ras signaling activation and AMPK modulation at environmentally relevant doses,^{15,17} our results extend this understanding by identifying specific molecular targets in the cholesterol biosynthetic pathway. The selective modulation we observed, characterized by enhanced HMGCR and FDFT1 protein expression without corresponding transcriptional changes, suggests a complex regulatory network distinct from previously reported mechanisms. Furthermore, our observation of modest changes in lipogenic enzymes coupled with tissue-specific insulin signaling perturbations raises important questions about the integrated metabolic response to TBBPA exposure, particularly in the context of previous findings showing TBBPA's effects on gut–liver axis and microbiome composition.¹⁶ These results not only provide mechanistic insights into TBBPA-induced metabolic disruption but also suggest potential therapeutic strategies targeting USP20 and HMGCR to mitigate these effects.

The prevalence of obesity has increased at an alarming rate; however, its etiology remains elusive.⁵¹ Notably, available data do not support the notion that higher energy consumption is a driving factor in the obesity epidemic.⁵² In 2002, researchers began to investigate the role of environmental compounds in the obesity epidemic.^{53,54} The potential contribution of environmental chemicals to obesity has been increasingly reported, with more than 15 chemical substances now identified as capable of inducing weight gain and altering glucose and lipid metabolism.⁵⁵ For instance, bisphenol A has been shown to cause ectopic fat accumulation and glucose intolerance.^{56,57} Monobenzyl phthalate (MBzP), mono-(2-ethyl-5-hydroxyhexyl) phthalate (MEHHP), mono-(2-ethyl-5-oxohexyl) phthalate (MEOHP), and monoethyl phthalate (MEP) have been associated with increased waist circumference, while monobutyl phthalate (MBP), MBzP, and MEP may reduce insulin sensitivity.⁵⁸ Our findings further corroborate that TBBPA can promote the development of obesity. This complex interplay between environmental factors and metabolic processes underscores the multifaceted nature of obesity etiology and highlights the need for a comprehensive

approach to understanding and addressing this global health challenge.

4. ENVIRONMENTAL IMPLICATIONS

Obesity-related metabolic disorders have emerged as a major global public health challenge, characterized by high prevalence rates, rapid growth, and far-reaching impacts. These conditions not only affect a vast population but also exhibit an accelerating spread, placing immense strain on healthcare systems worldwide. The influence of environmental pollutants on obesity has garnered increasing attention in recent years. Our research demonstrates that under conditions of high-energy dietary intake, environmental doses of TBBPA can further disrupt energy homeostasis through multiple mechanisms. TBBPA appears to interfere with the endocrine system, leading to a reduction in the BMR and an acceleration of insulin resistance development. Moreover, our findings reveal that TBBPA promotes cholesterol synthesis via the USP20-HMGCR pathway. Collectively, these effects significantly increase the risk of type 2 diabetes, fatty liver disease, and atherosclerosis. This study underscores the complex interplay among environmental pollutants, dietary factors, and metabolic health, highlighting the need for a multifaceted approach to address the growing obesity epidemic and its associated disorders.

■ ASSOCIATED CONTENT

Supporting Information

The Supporting Information is available free of charge at <https://pubs.acs.org/doi/10.1021/acs.est.4c12616>.

Antibodies used in the study and nucleotide sequences of the qPCR primers (PDF)

■ AUTHOR INFORMATION

Corresponding Author

Xiong-Jie Shi – Hubei Key Laboratory of Cell Homeostasis, College of Life Sciences, Wuhan University, Wuhan 430072, China; orcid.org/0000-0002-3750-6676; Email: xjshi@whu.edu.cn

Authors

Yi Ding – Hubei Key Laboratory of Cell Homeostasis, College of Life Sciences, Wuhan University, Wuhan 430072, China

Tingfu Zhang – Hubei Key Laboratory of Cell Homeostasis, College of Life Sciences, Wuhan University, Wuhan 430072, China

Hui-Bing Ma – Hubei Key Laboratory of Cell Homeostasis, College of Life Sciences, Wuhan University, Wuhan 430072, China

Jian Han – State Key Laboratory of Freshwater Ecology and Biotechnology, Institute of Hydrobiology, Chinese Academy of Sciences, Wuhan 430072, China; orcid.org/0000-0003-3930-0003

Wenzhuo Zhu – Hubei Key Laboratory of Cell Homeostasis, College of Life Sciences, Wuhan University, Wuhan 430072, China

Xiaolu Zhao – Hubei Key Laboratory of Cell Homeostasis, College of Life Sciences, Wuhan University, Wuhan 430072, China; orcid.org/0000-0003-1535-3880

Xiao-Yi Lu – Hubei Key Laboratory of Cell Homeostasis, College of Life Sciences, Wuhan University, Wuhan 430072, China

Bingsheng Zhou – State Key Laboratory of Freshwater Ecology and Biotechnology, Institute of Hydrobiology, Chinese Academy of Sciences, Wuhan 430072, China; orcid.org/0000-0003-0119-1868

Complete contact information is available at:

<https://pubs.acs.org/10.1021/acs.est.4c12616>

Notes

The authors declare no competing financial interest.

■ ACKNOWLEDGMENTS

This study was supported by the National Key Research and Development Program of China (2022YFA0806602, 2022YFC2502403, 2019YFA0802701) and the National Natural Science Foundation China (32271341, 22327901, 32271219).

■ REFERENCES

- (1) Alae, M.; Arias, P.; Sjödin, A.; Bergman, Å. An Overview of Commercially Used Brominated Flame Retardants, Their Applications, Their Use Patterns in Different Countries/Regions and Possible Modes of Release. *Environ. Int.* **2003**, *29* (6), 683–689.
- (2) Sunday, O. E.; Bin, H.; Guanghua, M.; Yao, C.; Zhengjia, Z.; Xian, Q.; Xiangyang, W.; Weiwei, F. Review of the Environmental Occurrence, Analytical Techniques, Degradation and Toxicity of TBBPA and Its Derivatives. *Environ. Res.* **2022**, *206*, No. 112594.
- (3) Yu, Y.; Wang, Z.; Wang, Q.; Xiang, M.; Zhang, Y.; Ge, Q.; Li, L.; Li, H.; Ma, R. Excretion Characteristics of Tetrabromobisphenol-A in Wistar Rats Following Mouth and Nose Inhalation Exposure. *Chemosphere* **2017**, *175*, 147–152.
- (4) Birnbaum, L. S.; Staskal, D. F. Brominated Flame Retardants: Cause for Concern? *Environ. Health Perspect.* **2004**, *112* (1), 9–17.
- (5) McAvoy, D. C.; Pittinger, C. A.; Willis, A. M. Biotransformation of Tetrabromobisphenol A (TBBPA) in Anaerobic Digester Sludge, Soils, and Freshwater Sediments. *Ecotoxicol. Environ. Saf.* **2016**, *131*, 143–150.
- (6) Ni, H. G.; Zeng, H. HBCD and TBBPA in Particulate Phase of Indoor Air in Shenzhen. *China. Sci. Total Environ.* **2013**, *458*–460, 15–19.
- (7) Zhou, H.; Yin, N.; Faiola, F. Tetrabromobisphenol A (TBBPA): A Controversial Environmental Pollutant. *J. Environ. Sci. (China)* **2020**, *97*, 54–66.
- (8) Miao, B.; Yakubu, S.; Zhu, Q.; Issaka, E.; Zhang, Y.; Adams, M. A Review on Tetrabromobisphenol A: Human Biomonitoring, Toxicity, Detection and Treatment in the Environment. *Molecules* **2023**, *28* (6), 2505.
- (9) Wu, Y.; Li, Y.; Kang, D.; Wang, J.; Zhang, Y.; Du, D.; Pan, B.; Lin, Z.; Huang, C.; Dong, Q. Tetrabromobisphenol A and Heavy Metal Exposure via Dust Ingestion in an E-Waste Recycling Region in Southeast China. *Sci. Total Environ.* **2016**, *541*, 356–364.
- (10) Shi, Z. X.; Wu, Y. N.; Li, J. G.; Zhao, Y. F.; Feng, J. F. Dietary Exposure Assessment of Chinese Adults and Nursing Infants to Tetrabromobisphenol-A and Hexabromocyclododecanes: Occurrence Measurements in Foods and Human Milk. *Environ. Sci. Technol.* **2009**, *43* (12), 4314–4319.
- (11) Zhu, B.; Zhao, G.; Yang, L.; Zhou, B. Tetrabromobisphenol A Caused Neurodevelopmental Toxicity via Disrupting Thyroid Hormones in Zebrafish Larvae. *Chemosphere* **2018**, *197*, 353–361.
- (12) Maur, G.; Edwards, B.; Habibi, H. R.; Allan, E. R. O. TBBPA Downregulates Thyroid Receptor and Estrogen Receptor mRNA Levels in Goldfish Gonadal Tissue. *Anim. Reprod. Sci.* **2022**, *240*, No. 106990.
- (13) Castro, L.; Liu, J.; Yu, L.; Burwell, A. D.; Saddler, T. O.; Santiago, L. A.; Xue, W.; Foley, J. F.; Staup, M.; Flagler, N. D.; Shi, M.; Birnbaum, L. S.; Dixon, D. Differential Receptor Tyrosine Kinase Phosphorylation in the Uterus of Rats Following Developmental

Exposure to Tetrabromobisphenol A. *Toxicology research and application* **2021**, *5*, 239784732110471.

- (14) Heindel, J. J.; Blumberg, B.; Cave, M.; Machtinger, R.; Mantovani, A.; Mendez, M. A.; Nadal, A.; Palanza, P.; Panzica, G.; Sargis, R.; Vandenberg, L. N.; vom Saal, F. Metabolism Disrupting Chemicals and Metabolic Disorders. *Reprod Toxicol* **2017**, *68*, 3–33.
- (15) Yao, L.; Wang, Y.; Shi, J.; Liu, Y.; Guo, H.; Yang, X.; Liu, Y.; Ma, J.; Li, D.; Wang, Z.; Li, Z.; Luo, Q.; Fu, J.; Zhang, Q.; Qu, G.; Wang, Y.; Jiang, G. Toxicity of Tetrabromobisphenol A and Its Derivative in the Mouse Liver Following Oral Exposure at Environmentally Relevant Levels. *Environ. Sci. Technol.* **2021**, *55* (12), 8191–8202.
- (16) Gomez, M. V.; Dutta, M.; Suvorov, A.; Shi, X.; Gu, H.; Mani, S.; Yue Cui, J. Early Life Exposure to Environmental Contaminants (BDE-47, TBBPA, and BPS) Produced Persistent Alterations in Fecal Microbiome in Adult Male Mice. *Toxicol. Sci.* **2021**, *179* (1), 14–30.
- (17) Lu, L.; Hu, J.; Li, G.; An, T. Low Concentration Tetrabromobisphenol A (TBBPA) Elevating Overall Metabolism by Inducing Activation of the Ras Signaling Pathway. *J. Hazard Mater.* **2021**, *416*, No. 125797.
- (18) Popkin, B. M.; Hawkes, C. Sweetening of the Global Diet, Particularly Beverages: Patterns, Trends, and Policy Responses. *Lancet Diabetes Endocrinol* **2016**, *4* (2), 174–186.
- (19) Malik, V. S.; Willet, W. C.; Hu, F. B. Nearly a Decade on - Trends, Risk Factors and Policy Implications in Global Obesity. *Nat. Rev. Endocrinol* **2020**, *16* (11), 615–616.
- (20) Blüher, M. Metabolically Healthy Obesity. *Endocr Rev.* **2020**, *41* (3), 405–420.
- (21) Kim, U. J.; Oh, J. E. Tetrabromobisphenol A and Hexabromocyclododecane Flame Retardants in Infant–Mother Paired Serum Samples, and Their Relationships with Thyroid Hormones and Environmental Factors. *Environ. Pollut.* **2014**, *184*, 193–200.
- (22) Cariou, R.; Antignac, J. P.; Zalko, D.; Berrebi, A.; Cravedi, J. P.; Maume, D.; Marchand, P.; Monteau, F.; Riu, A.; Andre, F.; Le Bizec, B. Exposure Assessment of French Women and Their Newborns to Tetrabromobisphenol-A: Occurrence Measurements in Maternal Adipose Tissue, Serum, Breast Milk and Cord Serum. *Chemosphere* **2008**, *73* (7), 1036–1041.
- (23) Zhu, Z. C.; Chen, S. J.; Zheng, J.; Tian, M.; Feng, A. H.; Luo, X. J.; Mai, B. X. Occurrence of Brominated Flame Retardants (BFRs), Organochlorine Pesticides (OCPs), and Polychlorinated Biphenyls (PCBs) in Agricultural Soils in a BFR-Manufacturing Region of North China. *Sci. Total Environ.* **2014**, *481* (1), 47–54.
- (24) He, M. J.; Luo, X. J.; Yu, L. H.; Wu, J. P.; Chen, S. J.; Mai, B. X. Diastereoisomer and Enantiomer-Specific Profiles of Hexabromocyclododecane and Tetrabromobisphenol A in an Aquatic Environment in a Highly Industrialized Area, South China: Vertical Profile, Phase Partition, and Bioaccumulation. *Environmental pollution* **2013**, *179*, 105–110.
- (25) Hill, J. O.; Wyatt, H. R.; Peters, J. C. The Importance of Energy Balance. *Eur. Endocrinol* **2013**, *9* (2), 111–115.
- (26) Yu, Y.; Hao, C.; Xiang, M.; Tian, J.; Kuang, H.; Li, Z. Potential Obesogenic Effects of TBBPA and Its Alternatives TBBPS and TCBCPA Revealed by Metabolic Perturbations in Human Hepatoma Cells. *Sci. Total Environ.* **2022**, *832*, No. 154847.
- (27) Wing, R. R.; Lang, W.; Wadden, T. A.; Safford, M.; Knowler, W. C.; Bertoni, A. G.; Hill, J. O.; Brancati, F. L.; Peters, A.; Wagenknecht, L. Benefits of Modest Weight Loss in Improving Cardiovascular Risk Factors in Overweight and Obese Individuals with Type 2 Diabetes. *Diabetes Care* **2011**, *34* (7), 1481–1486.
- (28) Ryan, D. H.; Yockey, S. R. Weight Loss and Improvement in Comorbidity: Differences at 5%, 10%, 15%, and Over. *Curr. Obes Rep* **2017**, *6* (2), 187–194.
- (29) Westerterp, K. R. Control of Energy Expenditure in Humans. *Eur. J. Clin Nutr* **2017**, *71* (3), 340–344.
- (30) Schutz, Y.; Ravussin, E. Respiratory Quotients Lower than 0.70 in Ketogenic Diets. *Am. J. Clin. Nutr.* **1980**, *33* (6), 1317–1319.
- (31) Ahmed, F.; Pereira, M. J.; Aguer, C. Bisphenols and the Development of Type 2 Diabetes: The Role of the Skeletal Muscle and Adipose Tissue. *Environments* **2021**, *8* (4), 35.
- (32) Boucher, J.; Kleinridders, A.; Ronald Kahn, C. Insulin Receptor Signaling in Normal and Insulin-Resistant States. *Cold Spring Harb. Perspect. Biol.* **2014**, *6* (1), a009191.
- (33) Sharabi, K.; Tavares, C. D. J.; Rines, A. K.; Puigserver, P. Molecular Pathophysiology of Hepatic Glucose Production. *Mol. Aspects Med.* **2015**, *46*, 21–33.
- (34) Petersen, M. C.; Vatner, D. F.; Shulman, G. I. Regulation of Hepatic Glucose Metabolism in Health and Disease. *Nat. Rev. Endocrinol* **2017**, *13* (10), 572–587.
- (35) Kurpad, A. V.; Khan, K.; Calder, A. G.; Elia, M. Muscle and Whole Body Metabolism after Norepinephrine. *Am. J. Physiol.* **1994**, *266* (6 Pt 1), E877–E884.
- (36) Morimoto, C.; Kameda, K.; Tsujita, T.; Okuda, H. Relationships between Lipolysis Induced by Various Lipolytic Agents and Hormone-Sensitive Lipase in Rat Fat Cells. *J. Lipid Res.* **2001**, *42* (1), 120–127.
- (37) Markussen, L. K.; Rondini, E. A.; Johansen, O. S.; Madsen, J. G. S.; Sustarsic, E. G.; Marcher, A. B.; Hansen, J. B.; Gerhart-Hines, Z.; Granneman, J. G.; Mandrup, S. Lipolysis Regulates Major Transcriptional Programs in Brown Adipocytes. *Nat. Commun.* **2022**, *13* (1), 3956.
- (38) Cero, C.; Lea, H. J.; Zhu, K. Y.; Shamsi, F.; Tseng, Y. H.; Cypess, A. M. B3-Adrenergic Receptors Regulate Human Brown/Beige Adipocyte Lipolysis and Thermogenesis. *JCI Insight* **2021**, *6* (11), No. e139160.
- (39) Villalobos-Labra, R.; Subiabre, M.; Toledo, F.; Pardo, F.; Sobrevia, L. Endoplasmic Reticulum Stress and Development of Insulin Resistance in Adipose, Skeletal, Liver, and Foetoplacental Tissue in Diabetes. *Mol. Aspects Med.* **2019**, *66*, 49–61.
- (40) Lu, X. Y.; Shi, X. J.; Hu, A.; Wang, J. Q.; Ding, Y.; Jiang, W.; Sun, M.; Zhao, X.; Luo, J.; Qi, W.; Song, B. L. Feeding Induces Cholesterol Biosynthesis via the MTORC1-USP20-HMGCR Axis. *Nature* **2020**, *588* (7838), 479–484.
- (41) Di Angelantonio, E.; Sarwar, N.; Perry, P.; Kaptoge, S.; Ray, K. K.; Thompson, A.; Wood, A. M.; Lewington, S.; Sattar, N.; Packard, C. J.; Collins, R.; Thompson, S. G.; Danesh, J.; Tipping, R. W.; Ford, C. E.; Pressel, S. L.; Walldius, G.; Jungner, I.; Folsom, A. R.; Chambless, L. E.; Panagiotakos, D. B.; Pitsavos, C.; Chrysohooou, C.; Stefanadis, C.; Knuiman, M.; Goldbourt, U.; Benderly, M.; Tanne, D.; Whincup, P. H.; Wannamethee, S. G.; Morris, R. W.; Kiechl, S.; Willeit, J.; Santer, P.; Mayr, A.; Wald, N.; Ebrahim, S.; Lawlor, D. A.; Yarnell, J. W. G.; Gallacher, J.; Casiglia, E.; Tikhonoff, V.; Nietert, P. J.; Sutherland, S. E.; Bachman, D. L.; Keil, J. E.; Cushman, M.; Psaty, B. M.; Tracy, R. P.; Tybjaerg-Hansen, A.; Nordestgaard, B. G.; Benn, M.; Frikke-Schmidt, R.; Giampaoli, S.; Palmieri, L.; Panico, S.; Vanuzzo, D.; Pilotto, L.; Gómez de la Cámara, A.; Gómez-Gerique, J. A.; Simons, L.; McCallum, J.; Friedlander, Y.; Fowkes, F. G. R.; Lee, A. J.; Smith, F. B.; Taylor, J.; Guralnik, J. M.; Phillips, C. L.; Wallace, R.; Guralnik, J.; Blazer, D. G.; Khaw, K. T.; Brenner, H.; Raum, E.; Müller, H.; Rothenbacher, D.; Jansson, J. H.; Wennberg, P.; Nissinen, A.; Donfrancesco, C.; Salomaa, V.; Harald, K.; Jousilahti, P.; Vartiainen, E.; Woodward, M.; D'Agostino, R. B.; Wolf, P. A.; Vasan, R. S.; Pencina, M. J.; Bladjberg, E. M.; Jørgensen, T.; Möller, L.; Jespersen, J.; Dankner, R.; Chetrit, A.; Lubin, F.; Rosengren, A.; Wilhelmsen, L.; Lappas, G.; Eriksson, H.; Björkelund, C.; Lissner, L.; Bengtsson, C.; Cremer, P.; Nagel, D.; Tilvis, R. S.; Strandberg, T. E.; Rodriguez, B.; Dekker, J. M.; Nijpels, G.; Stehouwer, C. D. A.; Rimm, E.; Pai, J. K.; Iso, H.; Noda, H.; Salonen, J. T.; Nyyssönen, K.; Tuomainen, T. P.; Deeg, D. J. H.; Poppelaars, J. L.; Meade, T. W.; Cooper, J. A.; Hedblad, B.; Berglund, G.; Engstrom, G.; Verschuren, W. M. M.; Blokstra, A.; Döring, A.; Koenig, W.; Meisinger, C.; Mraz, W.; Bas Bueno-de-Mesquita, H.; Kuller, L. H.; Grandits, G.; Selmer, R.; Tverdal, A.; Nystad, W.; Gillum, R.; Mussolino, M.; Rimm, E.; Hankinson, S.; Manson, J.; Knottenbelt, C.; Bauer, K. A.; Sato, S.; Kitamura, A.; Naito, Y.; Holme, I.; Nakagawa, H.; Miura, K.; Ducimetiere, P.; Jouven, X.; Crespo, C. J.; Garcia Palmieri, M. R.

- Amouyel, P.; Arveiler, D.; Evans, A.; Ferrieres, J.; Schulte, H.; Assmann, G.; Shepherd, J.; Packard, C. J.; Ford, I.; Cantin, B.; Lamarche, B.; Després, J. P.; Dagenais, G. R.; Barrett-Connor, E.; Wingard, D. L.; Bettencourt, R.; Gudnason, V.; Aspelund, T.; Sigurdsson, G.; Thorsson, B.; Trevisan, M.; Witteman, J.; Kardys, I.; Breteler, M.; Hofman, A.; Tunstall-Pedoe, H.; Tavendale, R.; Lowe, G. D. O.; Howard, B. V.; Zhang, Y.; Best, L.; Umans, J.; Ben-Shlomo, Y.; Davey-Smith, G.; Onat, A.; Njølstad, I.; Mathiesen, E. B.; Løchen, M. L.; Wilsgaard, T.; Ingelsson, E.; Lind, L.; Giedraitis, V.; Lannfelt, L.; Gaziano, J. M.; Stampfer, M.; Ridker, P.; Ulmer, H.; Diem, G.; Concin, H.; Tosetto, A.; Rodeghiero, F.; Marmot, M.; Clarke, R.; Collins, R.; Fletcher, A.; Brunner, E.; Shipley, M.; Buring, J.; Cobbe, S. M.; Robertson, M.; He, Y.; Marin Ibañez, A.; Feskens, E. J. M.; Kromhout, D.; Walker, M.; Watson, S.; Di Angelantonio, E.; Erqou, S.; Kaptoge, S.; Lewington, S.; Orfei, L.; Pennells, L.; Perry, P. L.; Ray, K. K.; Sarwar, N.; Alexander, M.; Wensley, F.; White, I. R.; Wood, A. M. Major Lipids, Apolipoproteins, and Risk of Vascular Disease. *JAMA* **2009**, *302* (18), 1993–2000.
- (42) Collins, R.; Reith, C.; Emberson, J.; Armitage, J.; Baigent, C.; Blackwell, L.; Blumenthal, R.; Danesh, J.; Smith, G. D.; DeMets, D.; Evans, S.; Law, M.; MacMahon, S.; Martin, S.; Neal, B.; Poulter, N.; Preiss, D.; Ridker, P.; Roberts, I.; Rodgers, A.; Sandercock, P.; Schulz, K.; Sever, P.; Simes, J.; Smeeth, L.; Wald, N.; Yusuf, S.; Peto, R. Interpretation of the Evidence for the Efficacy and Safety of Statin Therapy. *Lancet* **2016**, *388* (10059), 2532–2561.
- (43) Ding, Y.; Chen, Q.-B.; Xu, H.; Adi, D.; Ding, Y.-W.; Luo, W.-J.; Zhu, W.-Z.; Xu, J.-C.; Zhao, X.; Shi, X.-J.; Luo, J.; Yin, H.; Lu, X.-Y. siRNA Nanoparticle Targeting Usp20 Lowers Lipid Levels and Ameliorates Metabolic Syndrome in Mice. *J. Lipid Res.* **2024**, *65* (9), No. 100626.
- (44) Chang, T. Y.; Li, B. L.; Chang, C. C. Y.; Urano, Y. Acyl-Coenzyme A:Cholesterol Acyltransferases. *Am. J. Physiol Endocrinol Metab* **2009**, *297* (1), E1–9.
- (45) Wang, Y. J.; Bian, Y.; Luo, J.; Lu, M.; Xiong, Y.; Guo, S. Y.; Yin, H. Y.; Lin, X.; Li, Q.; Chang, C. C. Y.; Chang, T. Y.; Li, B. L.; Song, B. L. Cholesterol and Fatty Acids Regulate Cysteine Ubiquitylation of ACAT2 through Competitive Oxidation. *Nat. Cell Biol.* **2017**, *19* (7), 808–819.
- (46) Temel, R. E.; Hou, L.; Rudel, L. L.; Shelness, G. S. ACAT2 Stimulates Cholesteryl Ester Secretion in ApoB-Containing Lipoproteins. *J. Lipid Res.* **2007**, *48* (7), 1618–1627.
- (47) Wang, J. Q.; Li, L. L.; Hu, A.; Deng, G.; Wei, J.; Li, Y. F.; Liu, Y.; Bin, Lu, X. Y.; Qiu, Z. P.; Shi, X. J.; Zhao, X.; Luo, J.; Song, B. L. Inhibition of ASGR1 Decreases Lipid Levels by Promoting Cholesterol Excretion. *Nature* **2022**, *608* (7922), 413–420.
- (48) Cheng, V.; Volz, D. C. Halogenated Bisphenol a Analogues Induce PPARγ-Independent Toxicity within Human Hepatocellular Carcinoma Cells. *Curr. Res. Toxicol* **2022**, *3*, No. 100079.
- (49) Feng, X.; Zhang, L.; Xu, S.; Shen, A.-Z. ATP-Citrate Lyase (ACLY) in Lipid Metabolism and Atherosclerosis: An Updated Review. *Prog. Lipid Res.* **2020**, *77*, No. 101006.
- (50) Getz, G. S. Lipid Transfer Proteins: Introduction to the Thematic Review Series. *J. Lipid Res.* **2018**, *59* (5), 745–748.
- (51) Heindel, J. J.; Lustig, R. H.; Howard, S.; Corkey, B. E. Obesogens: A Unifying Theory for the Global Rise in Obesity. *Int. J. Obes (Lond)* **2024**, *48* (4), 449–460.
- (52) Mozaffarian, D. Perspective: Obesity-an Unexplained Epidemic. *Am. J. Clin. Nutr.* **2022**, *115* (6), 1445–1450.
- (53) Holtcamp, W. Obesogens: An Environmental Link to Obesity. *Environ. Health Perspect* **2012**, *120* (2), a62–a68.
- (54) Baillie-Hamilton, P. F. Chemical Toxins: A Hypothesis to Explain the Global Obesity Epidemic. *J. Altern Complement Med.* **2002**, *8* (2), 185–192.
- (55) Tang-Péronard, J. L.; Andersen, H. R.; Jensen, T. K.; Heitmann, B. L. Endocrine-Disrupting Chemicals and Obesity Development in Humans: A Review. *Obes Rev.* **2011**, *12* (8), 622–636.
- (56) Somm, E.; Schwitzgebel, V. M.; Toulotte, A.; Cederroth, C. R.; Combescur, C.; Nef, S.; Aubert, M. L.; Hüppi, P. S. Perinatal Exposure to Bisphenol a Alters Early Adipogenesis in the Rat. *Environ. Health Perspect* **2009**, *117* (10), 1549–1555.
- (57) Welshons, W. V.; Thayer, K. A.; Judy, B. M.; Taylor, J. A.; Curran, E. M.; vom Saal, F. S. Large Effects from Small Exposures. I. Mechanisms for Endocrine-Disrupting Chemicals with Estrogenic Activity. *Environ. Health Perspect* **2003**, *111* (8), 994–1006.
- (58) Stahlhut, R. W.; van Wijngaarden, E.; Dye, T. D.; Cook, S.; Swan, S. H. Concentrations of Urinary Phthalate Metabolites Are Associated with Increased Waist Circumference and Insulin Resistance in Adult U.S. Males. *Environ. Health Perspect* **2007**, *115* (6), 876–882.